# COOLING LOAD CALCULATION BY THE RADIANT TIME SERIES METHOD– EFFECT OF SOLAR RADIATION MODELS

**Alexandre M. S. Costa, amscosta@uem**
Universidade Estadual de Maringá, Av. Colombo 5790, Bloco 104, Maringá, PR, CEP 87020-900

***Abstract.*** *In this work was analyzed numerically the effect of three different models for solar radiation on the cooling load calculated by the radiant time series' method. The solar radiation models implemented were Clear sky, Isotropic sky and Anisotropic sky. The radiant time series' method(RTS) was proposed by ASHRAE (2001) for replacing the classical methods of cooling load calculation, such as TETD/TA. The method is based on computing the effect of space thermal energy storage on the instantaneous cooling load. The computing is carried out by splitting the heat gain components in convective and radiant parts. Following the radiant part is transformed using time series, which coefficients are a function of the construction type and heat gain (solar or non-solar). The transformed result is added to the convective part, giving the instantaneous cooling load. The method was applied for investigate the influence for an example room. The location used was –23$^o$ S and 51$^o$ W and the day was 21 of January, a typical summer day in the southern hemisphere. The room was composed of two vertical walls with windows exposed to outdoors with azimuth angles equals to west and east directions. The output of the different models of solar radiation for the two walls in terms of direct and diffuse components as well heat gains were investigated. It was verified that the clear sky exhibited the less conservative (higher values) for the direct component of solar radiation, with the opposite trend for the diffuse component. For the heat gain, the clear sky gives the higher values, three times higher for the peek hours than the other models. Both isotropic and anisotropic models predicted similar magnitude for the heat gain. The same behavior was also verified for the cooling load. The effect of room thermal inertia was decreasing the cooling load during the peak hours. On the other hand the higher thermal inertia values are the greater for the non peak hours. The effect of using walls with different thermal diffusivities attenuates and shifts the peaks of cooling load to later hours. Finally, for windows with glasses of different colors, thickness and films influences significativally the fenestration cooling loads.*

***Keywords****: cooling load, solar radiation models, radiant time series method, air conditioning, thermal comfort*

## 1. INTRODUCTION

The use of air conditioning was proven to be advantageous not only for human comfort, but also for controlling the environment (temperature, humidity and air quality) during processing of several products (e.g., electronics, pharmaceuticals, food, textiles and chemicals)..

One of the prior steps during the design of air conditioning systems is related to the calculations of energy requirements for keeping a zone in desirable temperature, humidity and air quality. Such calculations will be referred here as cooling load calculations.

Conversely, to the heat load calculation where only the steady state is considered, the cooling load calculation is transient and difficulted by the radiation mechanisms. These mechanisms encompass the radiation exchange between internal indoor surfaces and solar radiation through windows. The incoming radiation energy is absorbed and only after some time lag, is released to the indoor air as convective cooling load. The previous time lag is directly proportional to thermal inertia. In this way, the cooling load due to each heat gain component must take into account the thermal inertia effect. By his turn, solar radiation has important effects on both the heat gain and heat loss of a building. This effect depends to a great extent on both the location of the sun in the sky, the clearness of the atmosphere, weather conditions as well as on the nature and orientation of the building.

The computers advent in the second half of the last century, make possible the application of different methodologies for cooling load calculations. One of the most applied methodologies is the TETD/TA (total equivalent temperature differential method with time averaging). Originally presented in the 1967 ASHRAE Handbook of Fundamentals, this method does not require iterations and is convenient for spreadsheet implementation. On the other hand, its use is complicated by a number of empirical variables. Paying attention to these difficulties for the TETD/TA Spitler et al (1997) proposed a more rigourous and sequential method named radiant series method (RTS). Posterioryously, published by ASHRAE (2001), this method allows the quantifying the contribution of each component of heat gain and different construction materials on the total cooling load.

In the next section, we discuss shortly the fundamentals of the RTS method.

## 2. FUNDAMENTALS OF RADIANT TIMES SERIES METHOD

The RTS method is based in several simplifications of the heat balance method. Discussions of the heat balance method can be found in Pedersen et al (1998), Costa et al (2006) and Costa (2007). The simplifications of the RTS method are presented next.

- It is not performed a complete heat balance analysis for the exterior surfaces. The individual analysis of convection to the outdoor air, radiation to the environment and solar radiation, are replaced by a single heat transfer model, that involves the difference between the outdoor air temperature and an equivalent temperature. Such equivalent temperature is named sol-air temperature ;
- It is not performed a complete heat balance for the internal surfaces. Conversely, it is assumed that internal surfaces are at the same temperature of indoor air;
- It is not performed a complete heat balance for the indoor air.

Jointly, these simplifications allow the procedure to be performed step by step, with no simultaneous solution of the equations required as in the heat balance method.

In Fig. (1) the following five basic steps of the RTS method are diagrammed:

1- Determination of exterior boundary conditions.
2- Calculation of heat gains.
3- Splitting of heat gains into radiant and convective portions.
4- Determination of cooling loads due to the radiant and convective portion of heat gains.
5- Summation of loads due to convective and radiant portions of heat gains. See section 6 for details.

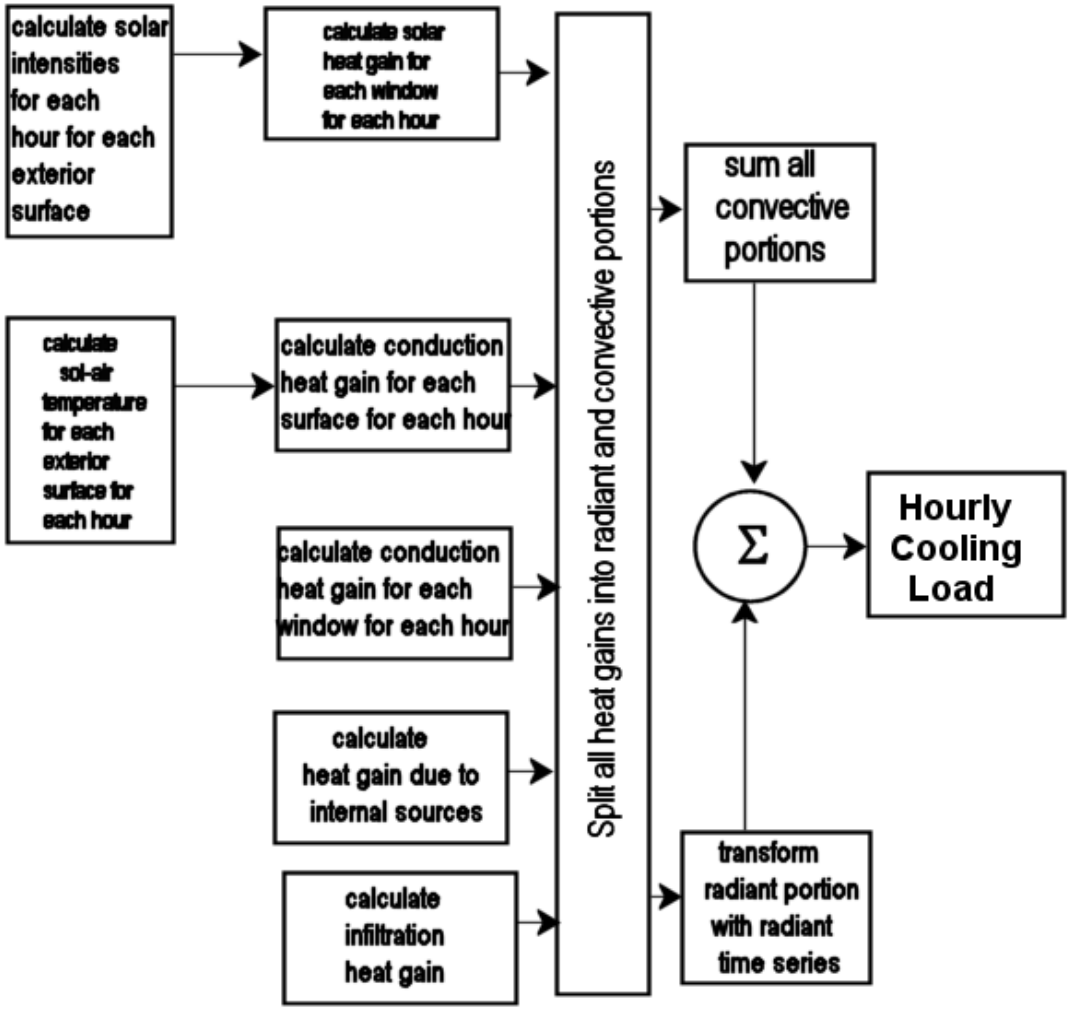


Figure 1. Diagram of radiant time series' method

Furthermore, for Fig. (1), some additional comments can be done:

The exterior boundary conditions are composed by the incident solar radiation and the sol-air temperature. The incident solar radiation is composed of direct, diffuse and reflected parcels, and are functions of angles related to the sun beam and surface location on Earth. In the next sections, is discussed the heat gain directly related to solar incidency : solar radiation models, sol air-temperature, and solar radiation through windows. A detailed discussion of the other heat gains can be found somewhere else (Costa, 2008 and Costa et al. 2008).

## 3 - SOLAR RADIATION MODELS

For cooling load calculations, it is very useful to know how to predict, for specified weather conditions, the solar irradiation of a surface at any given time and location. The direction from which diffuse radiation is received, that is, its distribution over the sky dome, is a function of considerably variable conditions, as cloudiness and atmospheric clarity. Meteorological data suggest the diffuse radiation model as being composed of three parts: isotropic part, received uniformly from the entire sky dome; circumsolar diffuse, concentrated in the part of the sky around the sun; and horizontal brightening, concentrated near the horizon.

### 3.1. Clear sky model

The first of solar radiation models employed in this study was the clear sky model. This model takes into account the absorption and scattering of solar radiation by atmosphere in cloudless days. Originally proposed by Hottel (1976), it is given by:

$$G_{cnb} = G_{on}\tau_b \tag{1}$$

$G_{cnb}$ is the clear sky normal beam radiation, i.e., direct radiation incident on a plane normal to the radiation direction.. Its units is W/m$^2$. It must be noticed that $G_{cnb}$ is equivalent to $G_{ND}$ given in ASHRAE Fundamentals Handbook. $G_{on}$ is the extraterrestrial radiation incident on the plane normal to radiation direction in the n$^{th}$ day of the year. Its value is function of solar constant $G_{sc}$ (1366 W/m$^2$) and given by (c.f. Duffie and Beckman, 2006):

$$G_{on} = G_{sc}\left(1 + 0.033\cos\left[\frac{360n}{365}\right]\right) \tag{2}$$

According to Hottel the atmospheric transmittance $\tau_b$ depends on the location altitude, $A$, in km, and sun´s zenite angle $\theta_z$ , as :

$$\tau_b = a_0 + a_1 \exp\left(-\frac{k}{\cos(\theta_z)}\right) \tag{3}$$

Where

$$a_0^* = 0.423 - 0.00821(6 - A)^2 \tag{4}$$

$$a_1^* = 0.5055 + 0.00595(6.5 - A)^2 \tag{5}$$

$$k^* = 0.2711 + 0.01858(2.5 - A)^2 \tag{6}$$

$$r_0 = \frac{a_0}{a_0^*} \quad r_1 = \frac{a_1}{a_1^*} \quad r_k = \frac{k}{k^*} \tag{7}$$

For the tropical climate type the following values are used : $r_0 = 0.95$ $r_1 = 0.98$ $r_k = 1.02$

$G_{cb}$ is the clear sky horizontal beam radiation., i.e., direct radiation incident on a horizontal plane

$$G_{cb} = G_{on}\tau_b \cos(\theta_z) \tag{8}$$

And for an arbitrarily tilted surface, the direct radiation $G_{cb,T}$ :

$$G_{cb,T} = G_{on}\tau_b \cos(\theta) \tag{9}$$

Where the incidence angle $\theta$, is the angle between the solar beam and the normal to the surface.
The relation between the beam (direct) radiation and the diffuse is given by Liu and Jordan (1960) as :

$$\tau_d = \frac{G_d}{G_{cnb}} = 0.271 - 0.294\,\tau_b \tag{10}$$

### 3.2. Estimating hourly total from daily total solar radiation

It must be pointed here, for the next two models of solar radiation some measured data of hourly total radiation $I$ [J/m$^2$] or daily total radiation $H$ [J/m$^2$] must be attainable. Moreover, it must be pointed up, that $I$ and $H$ are total measured values, i.e., the sum for a horizontal surface of direct and diffuse components of solar radiation . When only daily total data are available, an estimate of hourly total $I$ based on hourly total $H$ must be made. In this work, we employed the estimate by Collares-Pereira and Rabl (1979) based on statistical studies of several meteorological stations :

$$r_t = \frac{I}{H} \tag{11}$$

$$r_t = \frac{\pi}{24}\left(a + b\cos[\omega]\right)\frac{\cos[\omega]-\cos[\omega_s]}{\sin[\omega_s]-\frac{\pi\omega_s}{180}\cos[\omega_s]} \tag{12}$$

$$a = 0.409 + 0.5016\ \sin[\omega_s - 60] \tag{13}$$

$$b = 0.6609 - 0.4767\ \sin[\omega_s - 60] \tag{14}$$

In the above equations $\omega$ is the hour angle in degree for the time considered and $\omega_s$ is the hour angle for sunset. In addition, assuming hour uniformity, we used $G = I/3600$ s.

### 3.3. Isotropic sky model

First proposed by Liu and Jordan (1963), in this model the difuse component of solar radiation is treated as isotropic. For this model the diffuse component of solar radiation $I_d$ is given from eqs. (15) to (17).

Initially, is defined a clearness index $k_T$ :

$$k_T = \frac{I}{I_o} \equiv \frac{G}{G_o} \tag{15}$$

In the above equation $I$ is taken from measured hourly data or from daily data using Eq. (11)
The extraterrestrial radiation, $I_0$, on a horizontal surface for a given hour.

$$I_o = \frac{12 \bullet 3600}{\pi} G_{on}\left[\cos(\phi)\ \sin(\delta)\left(\sin(\omega_2)-\sin(\omega_1)\right)+\frac{\pi(\omega_2-\omega_1)}{180}\sin(\phi)\sin(\delta)\right] \tag{16}$$

$\phi$ and $\delta$ are the latitude and declination angles, respectivelly. $\omega_2$ and $\omega_1$ are the higher and lower, hour angles, respectivelly, that defines the given hour.

Once, $k_T$ is calculated the diffuse component $I_d$ is given by the Erbs et al. (1982) correlation:

$$\frac{I_d}{I} = \begin{cases} 1.0 - 0.09\ k_T & \text{for } k_T \le 0.22 \\ 0.9511 - 0.1604\ k_T + 4.388\ k_T^2 - 16.638\ k_T^3 + 12.366\ k_T^4 & \text{for } 0.22 \le k_T \le 0.8 \\ 0.165 & \text{for } k_T > 0.8 \end{cases} \tag{17}$$

The beam (direct) component of solar radiation for a horizontal surface is obtained by subtraction of total radiation $I$

$$I_b = I - I_d \tag{18}$$

For a arbitrarily tilted surface the ratio of cosine of incidence angle to the cosine of the zenith angle $R_b$ is given by:

$$R_b = \frac{\cos[\theta]}{\cos[\theta_z]} \tag{19}$$

Then, the total radiation $I_T$ for a tilted surface is the sum of a beam (direct), a diffuse isotropic and a reflected component as :

$$I_T = I_b R_b + I_d\left(\frac{1+\cos[\beta]}{2}\right)+I\,\rho_g\left(\frac{1-\cos[\beta]}{2}\right) \tag{20}$$

In the above equation, the second and third terms in parenthesis denotes the view factor between the surface and the sky; and the view factor between the surface and the ground. $\beta$ and $\rho_g$ are the slope angle and ground reflectivity, respectively.

### 3.4. Anisotropic sky model

This model considers an addition in the diffuse component in the circumsolar direction, near horizon brightness and cloudiness (Reindl et al, 1990). This is done using Eqs. (15) to (19), and the total solar radiation $I_T$ is given by :

$$I_T = \left( I_b + I_d \frac{I_b}{I_o} \right) R_b + I_d \left( 1 - \frac{I_b}{I_o} \right) \left( \frac{1+\cos[\beta]}{2} \right) \left[ 1 + \sqrt{\frac{I_b}{I}} \sin^3 \left[ \frac{\beta}{2} \right] \right] + I \rho_g \left( \frac{1-\cos[\beta]}{2} \right) \quad (21)$$

In the above equation, the first is the direct component, diffuse component and reflected component.

## 4 THE SOL-AIR TEMPERATURE

The sol-air temperature $t_e$ has origin on the energy balance for the external surface of an opaque wall. Its expression is given by :

$$t_e = t_o + \frac{\alpha G_t}{h_o} - \frac{\varepsilon \delta R}{h_o} \quad (22)$$

In the previous equation : the product of the external surface absortivity $\alpha$ and the total incident solar radiation $G_t$ represents the absorbed portion of solar radiation; $h_o$ and $t_o$ are the coefficients of heat convection and outdoor temperature, respectively; $\varepsilon \delta R$ represents the radiation exchange between the sky and surroundings and a blackbody at outside air temperature $t_o$.

## 5 - SOLAR HEAT GAINS THROUGH WINDOWS (FENESTRATION)

Typically the fenestration is associated with windows, their glazing materials, geometric form and shading devices. The solar radiation that strikes an unshaded window is divided between the reflected, absorbed and transmitted portion. In its turn, absorbed radiation is divided in an inward directed and an outward directed portion. Therefore, for windows the heat gain due to solar radiation is the sum of the transmitted $\dot{q}_{TSHGF}$ and inward directed portion $\dot{q}_{ASHGF}$, as given by:

$$\dot{q}_{TSHGF} = A_{SL} (SC) TSHGF_{SL} + A(SC) TSHGF_{SH} \quad (23)$$

$$\dot{q}_{ASHGF} = \left[ A_{SL} (SC) ASHGF_{SL} + A(SC) ASHGF_{SH} \right] N_i \quad (24)$$

In the previous equations *ASL* is the windows sunlit area and *ASH* is the shaded area; *A* is the total window area, $N_i$ is the inward flowing fraction of the absorbed radiation. *TSHGF*, stands for the transmitted solar heat gain factor, and represents the transmitted solar radiation that occurs in a unit area of standard (DSA) glass. Its units are given in W/m$^2$. Similarly, the absorbed solar heat gain factor *ASHGF* stands for the absorbed solar inward directed heat gain that occurs in a unit area of standard glass (DSA). The subscripts *SL* and *SH* for the transmited and absorbed heat gain factors, stands for sunlit and shaded situations, respectively. For the sunlit situation *TSHGF* depends on diffuse, and direct components of solar radiation, whereas for the shaded situation only the diffuse component rules. By his turn, procedures for estimating the solar heat gain assumes that a constant ratio exists between the solar heat gain through any given type of fenestration system and the solar heat gain through the standard (DSA) glass. *SC* abbreviates this ratio, called the shading coefficient.

In general, the transmitted radiant portion corresponds to the whole 100 % radiant portion. By his turn, the absorbed and inward oriented portion is splitted in 70 % radiant and 30% convective.

## 6 - THE RADIANT TIME SERIES

Before being added to the convective portion, the radiant portion of the heat gains is transformed by the radiant time series, given by :

$$\dot{q}_{r,\Theta} = r_0\dot{q}_{\Theta} + r_1\dot{q}_{\Theta-\delta} + r_2\dot{q}_{\Theta-2\delta} + r_3\dot{q}_{\Theta-3\delta} + \ldots + r_{23}\dot{q}_{\Theta-23\delta} \quad (25)$$

where,

$\dot{q}_{r,\Theta}$ cooling load for the current hour "θ"

$\dot{q}_{\Theta-n\delta}$ radiant portion of the heat gain corresponding to nδ hour ago

The coefficients $r_0$ , $r_1$, $r_2$, $r_3$, ..., $r_{23}$ are the radiant time series coefficients. They depend on the type of indoor environment and are classified according to their thermal inertia. Figure 2 presents a typical distribution of the coefficient values for high, medium and low thermal inertia. Figure 2 analysis shows that the coefficients for the low thermal inertia are important up to the 15th hour, decreasing after that. On the other hand, for media and high thermal inertia, the values are relevant up to the 19th and 22th hour, respectively. The previous behavior indicates that, for a indoor environment with low thermal inertia, only the first closest heat gain values to the current hour are relevant when applying Eq. (12).

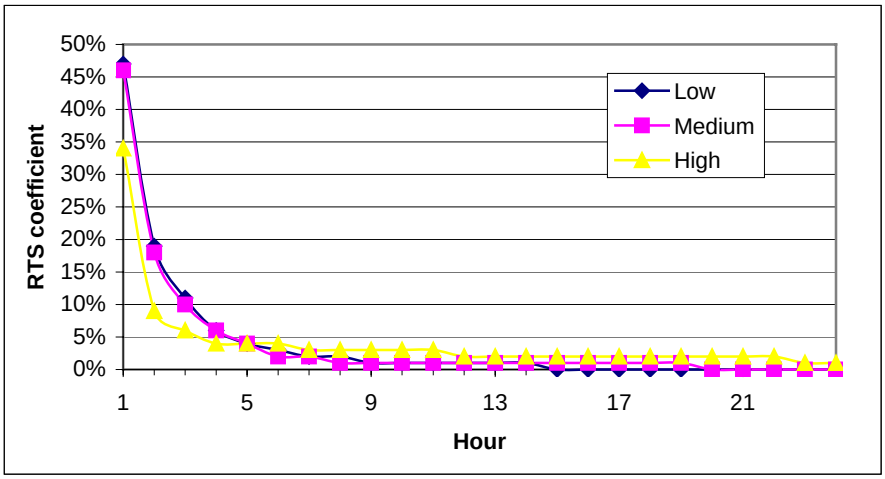


**Figure 2. Radiant time series coefficients**

## 7 - RESULTS

The method was applied for investigate numerically some influences for an example room. The room location was –23° S and 51° W and the day was 21 of January, a typical summer day in the southern hemisphere. The room was composed of two vertical walls with windows exposed to outdoors with azimuth angles equals to west and east directions. The indoor design temperature was 24 C and 50 % relative humidity. By his turn, the outdoor air temperature and humidity variation was based on meteorological data for the location. For the isotropic and anisotropic sky model, the daily total solar radiation for the location considered was based on Colle and Pereira (1998) solar data. For applying the radiant time series were employed the following values for the convective portions : 37 % for the conductive heat gains through walls and for the shaded windows areas; and 0 % for the sunlit areas. By his turn, the global heat transfer coefficient was 0.4 W $m^{-2}$ $C^{-1}$ for walls and 3.0 W $m^{-2}$ $C^{-1}$ for windows. For the walls the specific mass was 31 kg/$m^2$ and the thermal capacity 31 kJ $m^{-2}$ $C^{-1}$ .

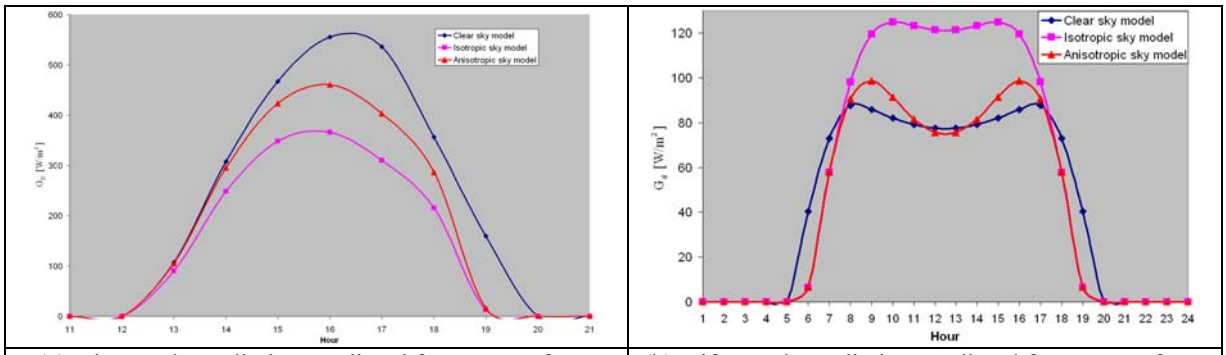


(a) Direct solar radiation predicted for west surfaces | (b) Difuse solar radiation predicted for west surfaces

Figure 3 – Predicted solar radiation components for west surfaces

In Fig. 3 is presented the incident solar radiation for the west surfaces predicted for the 3 different models. Analysis of Fig. 3(a) shows the direct component predicted by the clear sky model is the greatest, followed by the anisotropic sky and isotropic sky model. The Fig. 3 also shows the difference in intensity being greater near the peak hour. Figure 3(b) presents the behavior of the diffuse component. For hours between 7th and 15th hour all models predicted two maxima and a minimum value for the diffuse component. For the clear sky and isotropic model, the difference between the maximum and minimum is small and the profile for the diffuse radiation can be approximated coarsely as a square function. On the other hand, for the anisotropic the variation is greater. Finally, the curves comparison shows that for most of the hours between 7th and 15th hour the clear sky model predicted the lowest value followed by the anisotropic and clear sky model.

Figure 4 presents the incident solar radiation for east surfaces predicted for the three different models. From Fig. 4(a) the tendency verified in Fig. 3(a) for east surfaces, namely, the greates value for the clear sky, followed by the anisotropic sky and isotropic sky holds true for the west surfaces. In addition, the lowest values of direct components predicted for the east oriented as shown in Fig. 4(a) in comparison with west oriented can be interpreted as due to latitude location. Furthermore, for Fig. 4(b) the same analysis of Fig 3(b) holds true.

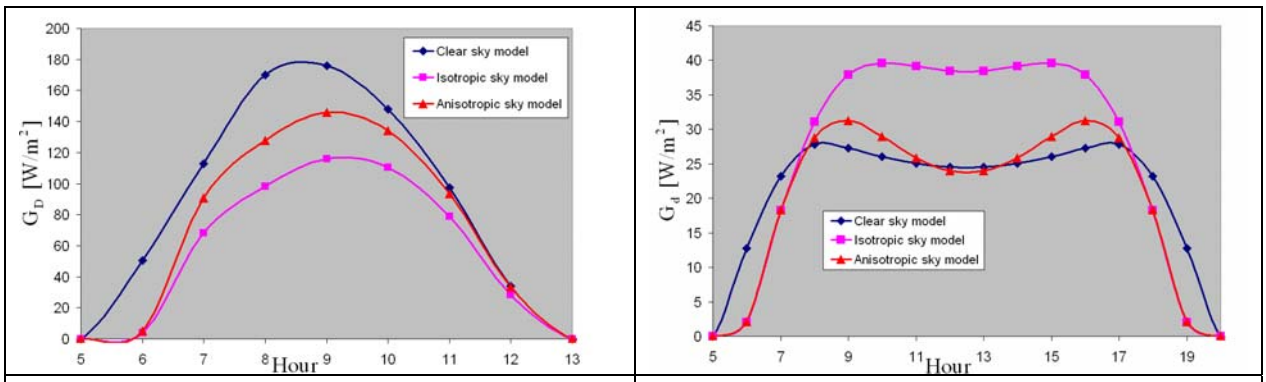


(a) Direct solar radiation predicted for the east wall | (b) Difuse solar radiation predicted for the east wall

Figure 4 – Predicted solar radiation components for the east wall

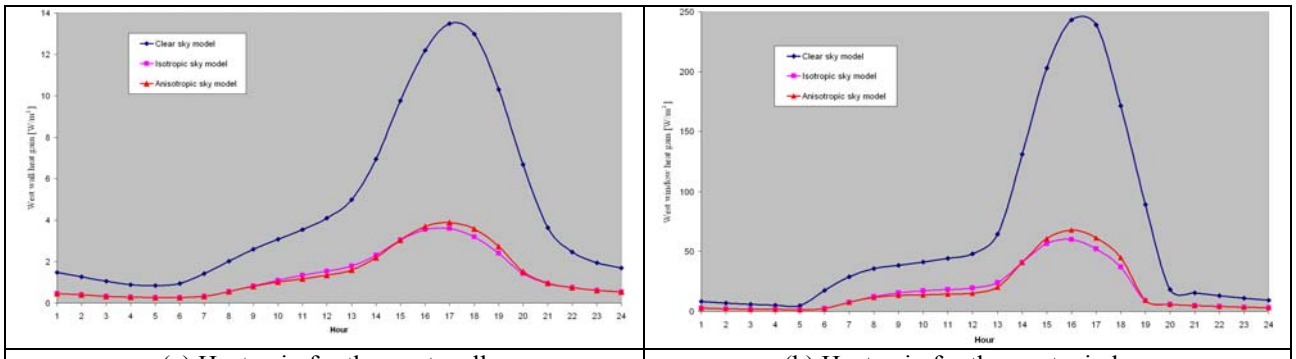


(a) Heat gain for the west wall | (b) Heat gain for the west window

Figure 5 Predicted heat gains for west surfaces

The heat gain per unitary area for the west wall and windows is presented in Fig. 5. In Fig. 5(a) and 5(b) the heat gain predicted using the clear sky model is the greatest and the values for the isotropic and anisotropic are slightly the same. The highest values of heat gains for the windows can be interpreted as due to the fact that glass expedite the solar radiation entering.

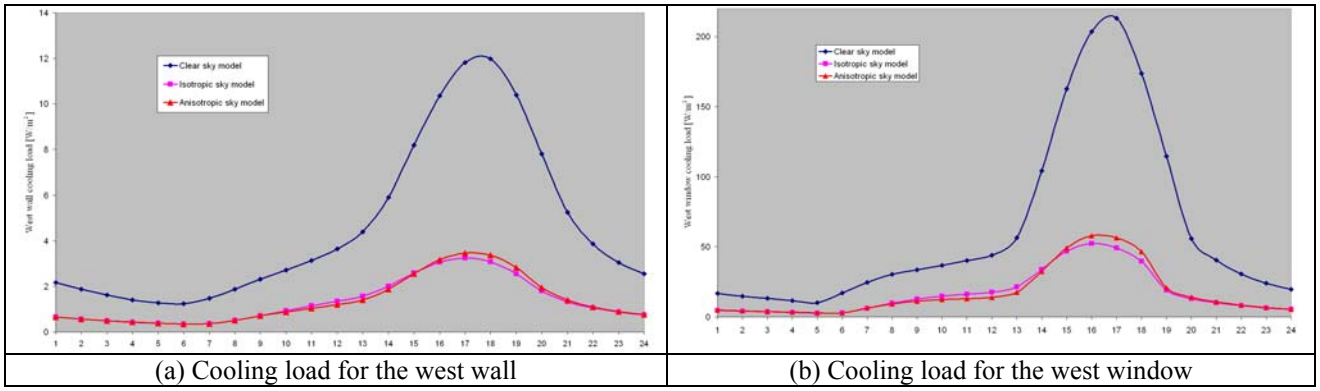


(a) Cooling load for the west wall (b) Cooling load for the west window

Figure 6 Predicted cooling loads for west wall and west window

The cooling load per unitary area for the west wall and windows is presented in Fig. 6. Analysis of Fig. 6, shows that the trend verified for heat gains is also verified for the cooling load (i.e., clear sky greatest, isotropic sky and anisotropic approximately the same). The cooling load is somewhat lower than the heat gain and the time period of peak values are the same.

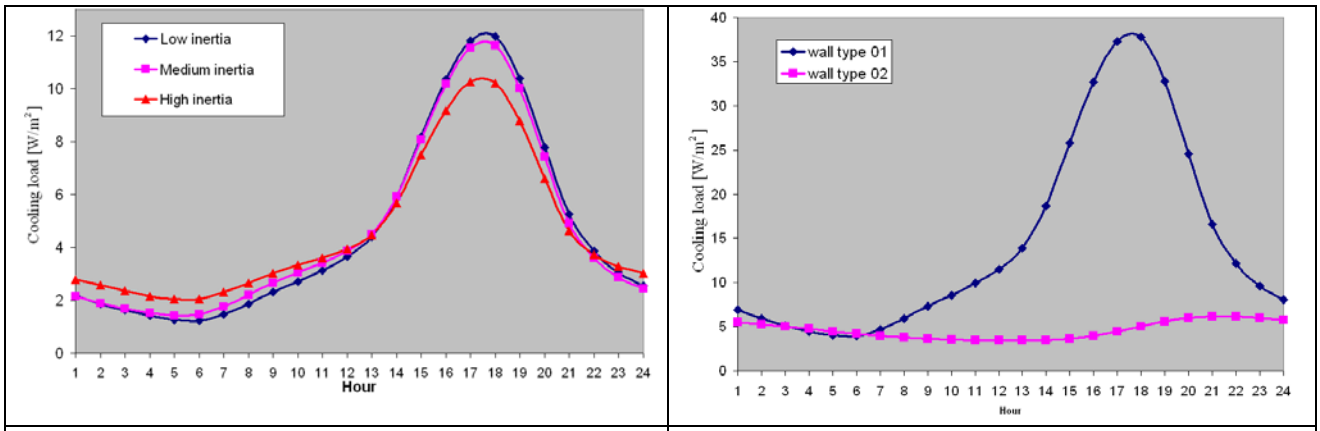


(a) Effect of indoor thermal inertia on the wall cooling load predicted by the clear sky model

(b) Effect of room wall type on the cooling load predicted by the clear sky model

Figure 7 – Predicted cooling load for different indoor thermal inertia and wall type.

In Fig. 7 is presented the effect of indoor thermal inertia and wall type on the cooling load predicted by the clear sky model. Analysis of Fig. 7(a) shows the effect of decreasing in cooling load with an increase of thermal inertia for hours near the peak values. Conversely, for the earlier hours, an analysis of Fig. 7(a) shows that the high thermal inertia produces the higher values of the cooling loads. Fig. 7(b) shows the effect of using walls with thermal diffusivities differing by a factor of 16. Analysis shows that wall type 01, with the higher value of thermal difusivity, predicts a peak value of cooling load seven times greater than the wall type 02 with the lower thermal difusivity. A shift in the time of the peak value is also seen for the lower thermal difusivity.

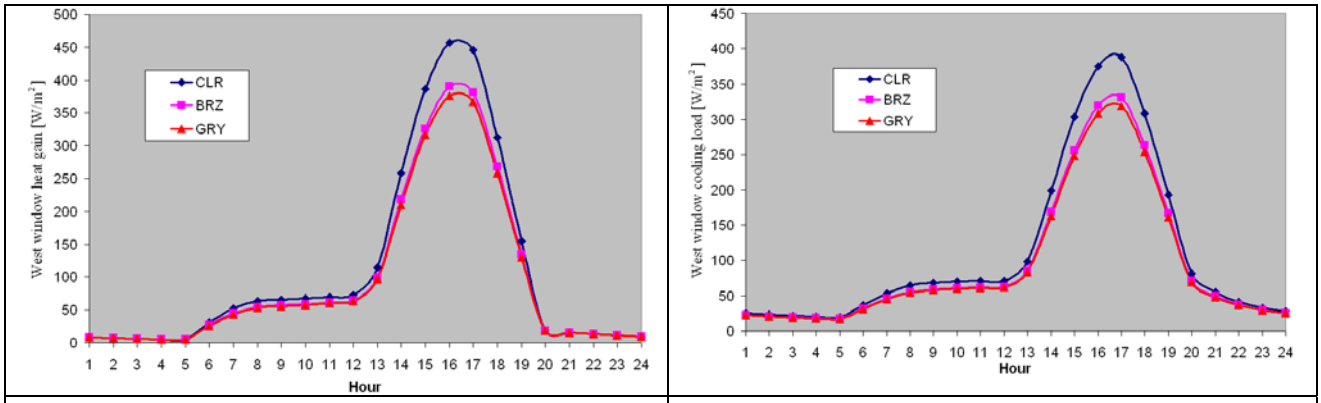


(a) Effect of window glass type on the heat gain

(b) Effect of window glass type on the cooling load

Figure 8 – Effect of window glass type

Figure 8 shows the effect of the windows glass type on heat gain and cooling load predicted using the clear sky model. The nomenclature CLR, BRZ, GRY stands for clear, bronze and gray tinted glasses, respectively. As it can be seen from Fig.8(a) and Fig 8(b) the lessening in the heat gain and cooling load is more distinct between the clear glass and tinted glasses than between two tinted glasses.

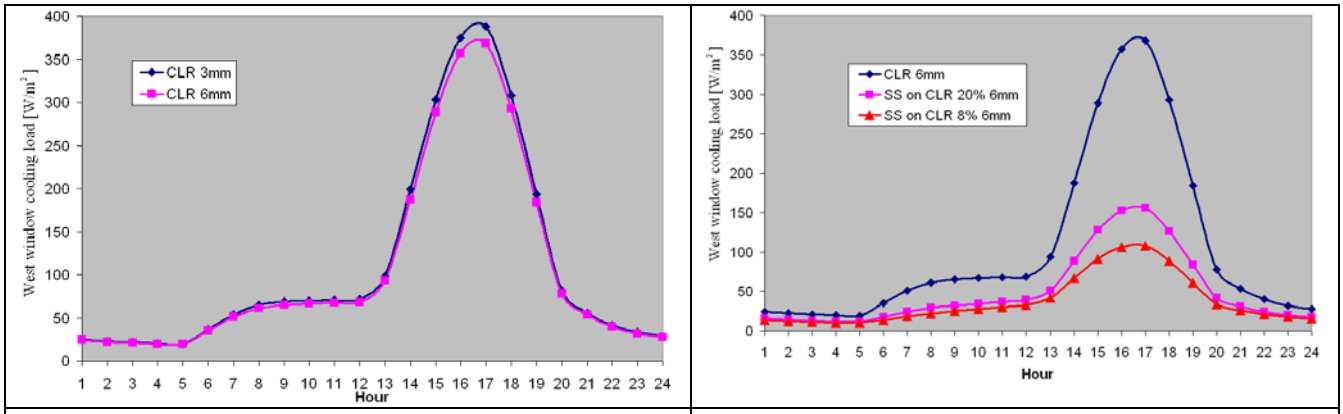


(a) Effect of window glass thickness on the west window cooling load

(b) Effect of windows coating on the west window cooling load

Figure 9 Effect of glass thickness and protective film

Figure 9 shows the influence of windows thickness and protective coatings on the cooling load. Analysis of Fig. 9(a) shows the thickness influences is only slimly relevant for the peak hour of the cooling load. On the other hand, the analysis of Fig. 9(b) shows that the use of protective coatings can decrease significantly the windows cooling load.

## 8 CONCLUSIONS

In this work, the effect of different parameters on the cooling load calculation using the RTS method was studied. The parametric study centered on using three different solar radiation models, room inertia, wall thermal diffusivities, glass thickness, glass color and protective coverings. The results show that the values for the direct component of solar radiation for the clear sky model are the greatest followed by the anisotropic, and isotropic sky model. For the diffuse component, the trend is flipped, with greatest values predicted by the isotropic sky, followed by the anisotropic sky and clear sky model. The results of the three solar models for the heat gain and cooling load shows that the use of clear sky model projects the higher values, up to 3.5 times greater than the other models for the peak values. The effect of room thermal inertia is higher peak values for the low inertia and smaller values for the low inertia for the earlier hours. The results also show the wall with higher thermal difusivities results and higher peak values. Finally, with regard to glass parameters, the results show the cooling load is slightly affected by thickness, more by color and strongly by protective covering.

## 9 REFERENCES

Costa, A. M. S., Takasse, N. B., Camin, R. V., Gonçalves, F. F., Drugovich, A. B., 2006, "Cálculo de carga térmica de resfriamento utilizando o método do balanço de calor- implementação no mathematica", IV Congresso Nacional de Engenharia Mecânica, Recife, Brazil.

Costa, A. M. S., 2007, "A study on the influence of the fenestration component on the cooling load calculation using the heat balance method", 19th International Congress of Mechanical Engineering, Brasília, Brazil.

Costa, A. M. S., 2008, "Cálculo de Carga Térmica pelo método da série radiante: efeito da inércia térmica e do coeficiente global de transferência de calor", Proceedings of MERCOFRIO 2008, Curitiba

Costa, A. M. S., Higa, M., Dainezi, J. C. 2008, Cálculo de Carga Térmica pelo método da série radiante: estudo de caso para as condições brasileiras, CONEM 2008, Salvador

Hottel, H. C., 1976, "A simple model for estimating the transmittance of Direct Solar Radiation through Clear Atmospheres", Solar Energy, 18, pp. 129-134

Duffie, J. A., Beckman, W. A., 2006, "Solar Engineering of Thermal Processes", Wiley; 3rd edition, 928p.

Collares-Pereira, M. and Rabl, A., 1979, "The average distribution of solar radiation- correlations between diffuse and hemispherical and between daily and hourly insolation values", Solar Energy, 22, pp. 155-164

Liu, B. Y. H., Jordan, R. C., 1960, "The interrelationship and characteristic distribution of direct, diffuse and total solar radiation", Solar Energy, 4(3), pp. 1-19

Liu, B. Y. H., Jordan, R. C., 1963, "The long term average performance of flat-plate solar energy collectors", Solar Energy, 7, pp. 53-74

Reindl, D. T., Beckman, W. A., Duffie, J. A., 1990, "Evaluation of Hourly Tilted Surface Radiation models", Solar Energy, 45, pp. 9-17

Erbs, D. G., S. A. Klein, Duffie, J. A., 1982, "Estimation of the diffuse radiation fraction for hourly, daily, and monthly average global radiation", Solar Energy, 28, pp. 293-302.

Mcquiston, F. C., Parker, J. D., Spitler, J., 2000, "Heating, ventilating, and air conditioning: analysis and design", John Wiley & Sons, USA, 623 p.

ASHRAE, 2001, "Handbook of Fundamentals", American Society of Heating, Refrigeration and Air Conditioning Engineers Inc., USA

ASHRAE, 1967, "Handbook of Fundamentals", American Society of Heating, Refrigeration and Air Conditioning Engineers Inc., USA

Pedersen, C. O., Fisher, D. E., Spitler, J. D., Liesen, R. J., 1998, "Cooling and heating load calculation principles", ASHRAE, USA.

Spitler, J. D., Fisher, D.E., Pedersen, C. O., 1997, "The radiant time series cooling load calculation procedure", ASHRAE Transactions, v. 103, n.2, pp. 503-515.

Colle, S., Pereira, E. B. (in portuguese), 1998, "Atlas de Radiação Solar do Brasil", Brasília, INMET - Instituto Nacional de Meteorologia, 57 p.

## 10. RESPONSIBILITY NOTICE

The author is the only responsible for the printed material included in this paper.